Nucleon Structure from Quenched Overlap Fermions

David Galletly^a, Martin Gürtler^b, Roger Horsley^a, Karl Koller^c, Volkard Linke^d, Paul E.L. Rakow^e, Charles J. Roberts^e, Gerrit Schierholz^b, Thomas Streuer^{*b}

^aUniversity of Edinburgh Edinburgh EH9 3JZ, UK DESY 05-177 Edinburgh 2005/13 PoS(LAT2005)36

^bJohn von Neumann-Institut für Computing NIC Platanenalleee 6, 15738 Zeuthen, Germany

^cSektion Physik, Universität München

80333 München, Germany

^d Institut für Theoretische Physik, Freie Universität Berlin 14196 Berlin, Germany

^eTheoretical Physics Division, Department of Mathematical Sciences, University of Liverpool Liverpool L69 3BX, UK

E-mail: galletly@ph.ed.ac.uk, martin.guertler@desy.de, rhorsley@ph.ed.ac.uk, karl.koller@lrz.uni-muenchen.de, volkard.linke@physik.fu-berlin.de, rakow@amtp.liv.ac.uk, cjr@amtp.liv.ac.uk, gerrit.schierholz@desy.de, thomas.streuer@desy.de

QCDSF Collaboration

We compute the lowest moments of the nucleon's structure functions using quenched overlap fermions at two different lattice spacings. The renormalisation is done nonperturbatively in the RI'-MOM-scheme.

XXIIIrd International Symposium on Lattice Field Theory 25-30 July 2005 Trinity College, Dublin, Ireland

^{*}Speaker.

1. INTRODUCTION

Information about the internal structure of the nucleon is encoded in its structure functions. While they cannot be computed directly on the lattice, the operator product expansion (OPE) provides a connection between their moments and nucleon matrix elements of local operators. For instance, for the unpolarised structure function F_1 , the OPE reads

$$2\int_0^1 dx x^{n-1} F_1(x, Q^2) = \sum_f E_{F_1, n}^{(f)} v_n^{(f)} + O(1/Q^2), \tag{1.1}$$

where f denotes the quark flavour, $E_{F_1,n}^{(f)}$ is the (perturbative) Wilson coefficient and the matrix element $v_n^{(f)}$ is defined by

$$\langle N(\vec{p})|O_{(f)}^{\{\mu_1...\mu_n\}} - \text{traces}|N(\vec{p})\rangle = 2\nu_n^{(f)}(p^{\mu_1}...p^{\mu_n} - \text{traces}),$$
 (1.2)

with the operator

$$O_{(f)}^{\mu_1\dots\mu_n} = \bar{\psi}_f \gamma^{\mu_1} \stackrel{\leftrightarrow}{D^{\mu_2}} \dots \stackrel{\leftrightarrow}{D^{\mu_n}} \psi_f. \tag{1.3}$$

Similar relations hold for the other structure functions, see e.g. [1] for details. Both the matrix element $v_n^{(f)}$ and the Wilson coefficient $E_{F_1,n}^{(f)}$ depend upon the choice of a renormalisation scheme and scale; only in their product, these dependencies cancel.

2. LATTICE SIMULATION

We use the overlap operator given by

$$D = \rho \left(1 + \frac{m_q}{2\rho} + \left(1 - \frac{m_q}{2\rho} \right) \gamma_5 \operatorname{sgn}(H_W(-\rho)) \right), \tag{2.1}$$

where $H_W(-\rho) = \gamma_5(D_W - \rho)$, D_W being the Wilson Dirac operator. We approximate the sign function appearing in (2.1) by minmax polynomials [2]. For the gauge part we chose the Lüscher-Weisz action [3]

$$S[U] = \frac{6}{g^2} \left(c_0 \sum_{\text{plaq}} \frac{1}{3} \text{Re Tr} \left[1 - U_{\text{plaq}} \right] + c_1 \sum_{\text{rect}} \frac{1}{3} \text{Re Tr} \left[1 - U_{\text{rect}} \right] + c_2 \sum_{\text{par}} \frac{1}{3} \text{Re Tr} \left[1 - U_{\text{par}} \right] \right), \quad (2.2)$$

with coefficients c_1 , c_2 ($c_0 + 8c_1 + 8c_2 = 1$) taken from tadpole improved perturbation theory [4]. We ran our computations at two lattice spacings, see table 1. The scale has been set from the pion decay constant, details are given in [5]. The parameter ρ in (2.1) was set to 1.4.

V	β	a(fm)	confs.
16^332	8.00	0.153(3)fm	300
24^348	8.45	0.105(2)fm	200

Table 1: Parameters of the gauge configurations used.

In order to remove O(a) errors from the three-point functions, we employ the method of [6], which amounts to replacing propagators $D^{-1}\Psi$ by $\frac{1}{1-\frac{m}{2\rho}}D^{-1}\Psi - \frac{1}{2(1-\frac{m}{2\rho})}\Psi$. Jacobi smeared point sources [1] with parameters $N_s = 50$ and $\kappa_s = 0.21$ have been used in order to obtain a good overlap with the ground state.

The computation of matrix elements follows the procedure outlined in [1]: We form the ratio

$$R = \frac{\langle N(t_{sink})O(\tau)\bar{N}(t_{source})\rangle}{\langle N(t_{sink})\bar{N}(t_{source})\rangle},$$
(2.3)

from which the matrix element can be extracted in the region $t_{source} < \tau < t_{sink}$. We always set $t_{source} = 0$ and $t_{sink} = 9$ ($t_{sink} = 13$) on the $\beta = 8.0$ ($\beta = 8.45$) configurations (in lattice units), which corresponds to a distance between source and sink of 1.4 fm.

The matrix elements we are considering are listed in table 2, along with the operators used for their determination, where we use the operators (1.3) and

$$O_{5,(f)}^{\mu_1\dots\mu_n} = \bar{\psi}_f \gamma_5 \gamma^{\mu_1} \stackrel{\leftrightarrow}{D^{\mu_2}} \dots \stackrel{\leftrightarrow}{D^{\mu_n}} \psi_f. \tag{2.4}$$

We compute only flavour non-singlet matrix elements, since in this case there is no contribution from disconnected diagrams.

3. NON-PERTURBATIVE RENORMALISATION

The operators appearing inside the three-point functions have to be renormalised. For $g_A = \Delta u - \Delta d$, the operator to be used is the axial current A_{μ} , the renormalisation of which is particularly simple because it does not depend on a renormalisation scheme or scale. It can be obtained from a Ward identity [7] as

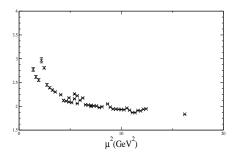
$$Z_A = \lim_{m_q \to 0} \lim_{t \to \infty} \frac{2m_q}{m_\pi} \frac{\langle P(t)P(0) \rangle}{\langle A_4(t)P(0) \rangle}.$$
 (3.1)

The renormalisation constants of the other operators under consideration are logarithmically divergent. We have computed them in the RI' – MOM-scheme [8]. In this scheme, the renormalisation condition is formulated in terms of quark Greens functions in Landau gauge with an operator insertion at zero momentum transfer:

$$C_O(p) = \frac{1}{V} \sum_{x,y,z} e^{-ip(x-y)} \langle \psi(x) O(z) \bar{\psi}(y) \rangle. \tag{3.2}$$

Matrix Element	Operator	
g_A	$ar{\psi}\gamma^5\gamma^2\psi$	
g_T	$ar{\psi}\gamma^5\sigma^{24}\psi$	
v_2	$O^{44} - \frac{1}{3} \left(O^{11} + O^{22} + O^{33} \right)$	
a_1	$\frac{1}{2}\left(O_5^{24}+O_5^{42}\right)$	

Table 2: Operators used in the three-point functions.



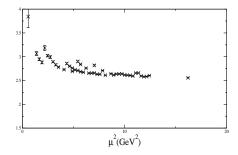


Figure 1: Left: The renormalisation constant $Z_{\nu_{2b}}^{RI'-MOM}(\mu)$, Right: The same, but with the renormalisation group running removed according to (3.6).

From this quantity, the amputated vertex function Γ_O is formed:

$$\Gamma_O(p) = S^{-1}(p)C_O(p)S^{-1}(p),$$
(3.3)

with the quark propagator

$$S(p) = \frac{1}{V} \sum_{x,y} e^{-ip(x-y)} \langle \psi(x)\bar{\psi}(y) \rangle. \tag{3.4}$$

The renormalisation condition at scale μ is

$$Z_{\psi}(\mu)Z_{O}(\mu)\Pi_{O}(\Gamma_{O}(p))\big|_{p^{2}=\mu^{2}}=1,$$
 (3.5)

with the projector $\Pi_O(\Gamma) = \frac{1}{12} \text{tr} \left(\Gamma_{O,\text{Born}}^{-1}(p) \Gamma \right)$. The wavefunction renormalisation constant Z_{ψ} has been determined from the relation $Z_{\psi} Z_A \Pi_A \left(\Gamma_A \right) = 1$.

In order to convert the results to the $\overline{\rm MS}$ -scheme, we first determine the renormalisation group invariant renormalisation constant $Z_O^{\rm RGI}$:

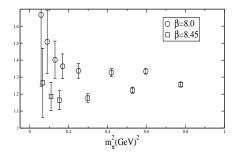
$$Z_O^{\text{RGI}} = \left(Z_O^{\text{RI}'-\text{MOM},\text{RGI}}(\mu)\right)^{-1} Z_O^{\text{RI}'-\text{MOM}}(\mu),$$
 (3.6)

and then convert to the $\overline{\rm MS}$ -scheme at scale μ' (we always use $\mu'=2{\rm GeV}$): $Z_O^{\overline{\rm MS}}(\mu')=Z_O^{\overline{\rm MS},{\rm RGI}}(\mu)Z_O^{{\rm RGI}}$ with the conversion functions

$$Z_O^{\mathscr{S},\text{RGI}}(\mu) = \left(2b_1 g^{\mathscr{S}}(\mu)^2\right)^{-\frac{d_{O,1}}{2b_1}} \exp\left[\int_0^{g^{\mathscr{S}}(\mu)} d\xi \left(\frac{\gamma_O^{\mathcal{S}}(\xi)}{\beta^{\mathcal{S}}(\xi)} + \frac{d_{O,1}}{b_1 \xi}\right)\right]. \tag{3.7}$$

The coefficients of the β and γ functions are taken from [9, 10].

In fig. 1 we plot $Z_{\nu_{2b}}^{RI'-MOM}$ and $Z_{\nu_{2b}}^{RGI}$ for $\beta=8.45$. From the latter plot, we read off $Z_{\nu_{2b}}^{RGI}=2.6$ from the plateau region $8\text{GeV}^2< p^2<15\text{GeV}^2$. Using $Z_{\nu_{2b}}^{\overline{\text{MS}},RGI}(2\text{GeV})=0.737$, we obtain $Z_{\nu_{2b}}^{\overline{\text{MS}}}=1.92$. The renormalisation constants for all operators we need are shown in table 3. A comparison with results obtained in one-loop tadpole-improved lattice perturbation theory [11, 12] shows large discrepancies, especially for the operators with one derivative.



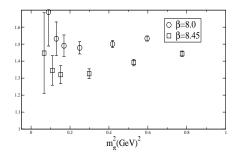


Figure 2: The nucleon's axial charge (left plot) and tensor charge (right plot) as a function of the squared pion mass

4. RESULTS

Our results for the axial charge g_A are displayed in fig. 2 (left). A linear extrapolation to the chiral limit yields $g_A = 1.37(5)$ at $\beta = 8.0$ and $g_A = 1.14(5)$ at $\beta = 8.45$. The tensor charge $g_T = \delta u - \delta d$ is plotted in fig. 2 (right); in this case, linear extrapolations to $m_q = 0$ yield $g_T = 1.35(4)$ at $\beta = 8.0$ and $g_T = 1.18(5)$ at $\beta = 8.45$.

The results for the matrix elements $v_2^{u-d} = \langle x \rangle^{u-d}$ and $a_1^{u-d} = 2\langle x \rangle^{\Delta u - \Delta d}$ are shown in fig. 3, together with the phenomenological values. In both cases, there is almost no dependence on the quark mass visible. In the range $m_\pi \gtrsim 400 \text{MeV}$, our results agree with previous results obtained from improved Wilson fermions [1].

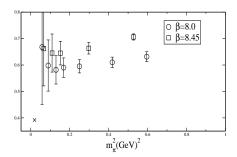
5. CONCLUSIONS

We have determined the flavour non-singlet nucleon matrix elements g_A , g_T , v_2 and a_1 from quenched overlap fermions. The renormalisation has been done nonperturbatively. Comparing the results at the two values for the lattice spacing we have, we find significant discretisation effects, in contrast with the situation for hadron masses [5].

While our results are in good agreement with earlier determinations, there remains a rather

Operator	$\beta = 8.0$		$\beta = 8.45$	
Operator	pert.	nonp.	pert.	nonp.
$O_{A_{\mu}}$	1.36	1.59	1.30	1.42
O_{g_T}	1.36	1.73	1.33	1.54
O_{v_2}	1.33	2.11	1.39	1.92
O_{a_1}	1.34	2.21	1.40	1.98

Table 3: Comparison between the renormalisation constants $Z_O^{\overline{\rm MS}}(2{\rm GeV})$ obtained non-perturbatively and in lattice perturbation theory.



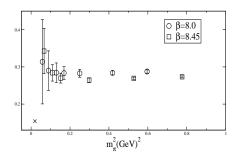


Figure 3: The nucleon matrix elements a_1^{u-d} (left plot) and v_2^{u-d} (right plot) as functions of the squared pion mass ($\overline{\text{MS}}$, 2GeV).

large discrepancy to the phenomenological values for v_2 and a_1 , even at the lowest quark masses we can reach at present.

ACKNOWLEDGEMENTS

The numerical calculations were performed at the HLRN (IBM pSeries 690), at NIC Jülich (IBM pSeries 690) and at the PC farms at DESY Zeuthen and LRZ Munich. We thank these institutions for their support. Part of this work is supported by DFG under contract FOR 465 (Forschergruppe Gitter-Hadronen-Phänomenologie)

References

- [1] M. Göckeler, R. Horsley, E.-M. Ilgenfritz, P. Rakow, G. Schierholz, A. Schiller, *Phys. Rev.* **D53** (1996) 2317.
- [2] L. Giusti, M. Lüscher, P. Weisz, H. Wittig, Comp. Phys. Comm. 153 (2003) 31.
- [3] M. Lüscher, P. Weisz, Comm. Math. Phys. 97 (1985) 59.
- [4] C. Gattringer, R. Hoffmann, S. Schaefer, Phys. Rev. **D65** (2002) 094503.
- [5] M. Gürtler et al., PoS (LAT2005) 077.
- [6] S. Capitani, M. Göckeler, R. Horsley, P.E.L. Rakow, H. Perlt, G. Schierholz, A. Schiller, *Phys. Lett.* **B468** (1999) 150.
- [7] L. Giusti, C. Hoelbling, C. Rebbi, Nucl. Phys. Proc. Suppl. 106 (2002) 739.
- [8] G. Martinelli, C. Pittori, C. T. Sachrajda, M. Testa and A. Vladikas, Nucl. Phys. B 445 (1995) 81.
- [9] J. A. Gracey, Nucl. Phys. B 662 (2003) 247.
- [10] J. A. Gracey, Nucl. Phys. B 667 (2003) 242.
- [11] R. Horsley, H. Perlt, P. E. L. Rakow, G. Schierholz and A. Schiller [QCDSF Collaboration], *Nucl. Phys. B* **693** (2004) 3 [Erratum-ibid. B **713** (2005) 601].
- [12] R. Horsley, H. Perlt, P. E. L. Rakow, G. Schierholz and A. Schiller [QCDSF Collaboration], arXiv:hep-lat/0505015.